Putting light in a spin

A. Dudley[a], R. Rop[b,c], I.A. Litvin[a], C. Lopez-Mariscal[d], F.S. Roux[a] and A. Forbes*[a,e,f]
[a]CSIR National Laser Centre, PO Box 395, Pretoria 0001, South Africa;
[b]Department of Physics, Moi University, PO Box 1125, Egerton 30100, Kenya;
[c]Department of Physics, Egerton University, PO Box 536, Eldoret 20115, Kenya;
[d]US Naval Research Laboratories, 4555 Overlook Ave. SW, Washington, DC 20375, USA;
[e]School of Physics, University of KwaZulu-Natal, Private Bag X54001, Durban 4000, South Africa;
[f]Stellenbosch University, Private Bag X1, Matieland 7602, South Africa.
Corresponding author: aforbes1@csir.co.za

ABSTRACT

We experimentally generated superpositions of higher-order Bessel beams that possess no global orbital angular momentum (OAM), yet exhibit an angular rotation in their intensity profile as the field propagates. The digital holograms encoded on a spatial light modulator (SLM), used for generating such fields, consist of two annular rings of unequal radial wave-vectors where each ring is encoded with an azimuthal mode of equal order but opposite charge. We present experimentally measured angular rotation rates for some example superposition fields, which are shown to be in good agreement with that predicted theoretically. Introducing a second SLM and a Fourier transforming lens, we demonstrate a simple approach to perform an azimuthal decomposition of our generated optical fields. Bounding the match-filter to an annular ring, of varying radius, we are able to perform a scale-independent azimuthal decomposition of our initial field. From the measured weightings of the azimuthally decomposed modes we show reconstruction of the cross-sectional intensity profile and OAM density of our initial field.

Keywords: Bessel beams, angular rotation, azimuthal decomposition, orbital angular momentum density

1. INTRODUCTION

The OAM of an optical field is associated with the azimuthal phase dependence of the field's wavefront. It was first shown that Laguerre-Gaussian (LG) laser modes contain a phase singularity[1], around which the phase of the field increases azimuthally, $\exp(il\theta)$, where l indicates the azimuthal mode index and θ is the azimuthal angle. Any optical field that possesses a helical phase structure, such as higher-order Bessel beams, carry OAM.

Zero-order and higher-order Bessel beams have received increased attention over the past few years due to their non-diffracting and self-reconstructing properties[2]. Durnin first illustrated that a zero-order Bessel beam can be generated by illuminating an annular ring, placed in the back focal plane of a lens, with a plane wave[3]. Many techniques exist for the generation of both zero and higher-order Bessel beams, such as refractive axicons[4-7] and diffractive computer generated holograms[8-13].

In this paper we extend Durnin's annular ring experiment by introducing two azimuthal modes at different radial positions to produce superpositions of higher-order Bessel beams[14,15]. The transverse intensity profiles of the resulting superimposed fields exhibit an interesting feature: they rotate about the propagation axis[14,15]. Other forms of rotating optical fields have been theoretically and experimentally realized as superpositions of higher-order Bessel beams[16-19], LG beams[17,20] and multi-mode hyper-geometric beams[17]. We report quantitative, experimental measurements of the rotation rates of superimposed higher-order Bessel beams and illustrate that the rotation rate is dependent on two parameters: the azimuthal modes and radial wave-vectors.

An understanding of the structure and propagation characteristics of different forms of laser modes has been achieved through the use of modal decomposition techniques[21-24]. Some techniques have employed a mode-multiplexing scheme encoded in computer generated holograms for the modal decomposition of laser beams from fibres[25-29]. Although these

Laser Beam Shaping XIII, edited by Andrew Forbes, Todd E. Lizotte, Proc. of SPIE Vol. 8490, 84900A

techniques are noteworthy, they require the scale parameter of the mode under investigation to be known for the fabrication of the diffractive optical element

In this paper we formulate a scale-independent, azimuthal decomposition of an arbitrary laser mode by making use of the angular harmonics of basis functions to express the spatial distribution in terms of spatially dependent coefficients[30]. We implement our measurement technique to infer the cross-sectional intensity profile of our initial superposition field, as well as its OAM density.

2. THEORY

A digital annular ring hologram (such as that in Fig. 1(a)), having the following transmission function

$$t(r,\theta)=\begin{cases}\exp(il\theta) & R_1-\dfrac{\Delta}{2}\le r\le R_1+\dfrac{\Delta}{2}\\ \exp(-il\theta) & R_2-\dfrac{\Delta}{2}< r\le R_2+\dfrac{\Delta}{2},\\ 0 & elsewhere\end{cases} \tag{1}$$

is encoded onto a SLM (in the form of Fig. 1(b)) and illuminated with an expanded Gaussian beam. R_1 and R_2 are the radii of each of the two annular rings, respectively and Δ is the width of both annular rings.

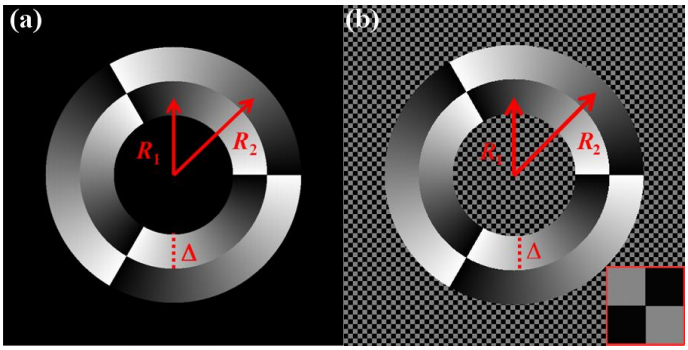

Figure 1. (a) The transmission function described in Eq. (1) for an azimuthal mode index of l = 3. (b) The digital hologram encoded on a phase-only SLM to execute both amplitude and phase modulations in a single step. The inset in (b) shows a 'zoomed-in' section of the alternating phase values of 0 and π, which mimic an amplitude mask of zero transmission[31].

The field in the Fourier plane of the digital annular ring hologram, described by the transmission function in Eq. (1), is determined by making use of the Kirchoff-Huygens diffraction integral, resulting in the contribution from the inner and outer annular rings to produce the following superposition[14]

$$A(r,\theta,z)=J_l(k_{1r}r)\exp(il\theta)\exp(ik_{1z}z)+J_{-l}(k_{2r}r)\exp(-il\theta)\exp(ik_{2z}z). \tag{2}$$

k_{1r} and k_{2r} denote the transverse wave-numbers, associated with each of the two Bessel beams, defined as $k_{1r}=k\sin\alpha_1$ and $k_{2r}=k\sin\alpha_2$, where $k=2\pi/\lambda$ and α is the opening angle of the cone on which the wave-vectors, produced by each annular ring, propagate. The longitudinal wave-numbers, k_{1z} and k_{2z}, are defined as $k_{1z}=k\cos\alpha_1$ and $k_{2z}=k\cos\alpha_2$.

Since the annular rings are arbitrarily thin and close to one another ($k_{1r}\approx k_{2r}=k_r$), this results in $J_l(k_{1r}r)\approx J_l(k_{2r}r)=J_l(k_rr)$ and by implementing the Bessel function identity, $J_{-l}(k_{2r}r)=(-1)^lJ_l(k_{2r}r)$, the intensity of the superimposed Bessel field is determined as

$$I(r,\theta,z)\propto 2J_l^2(k_rr)\left[(-1)^l+1+2(-1)^l\cos(k_{1z}z-k_{2z}z+2l\theta)\right] \tag{3}$$

The intensity profile (Eq. (3)) is modulated in the azimuthal co-ordinate, θ, by the function $\cos(2l\theta)$, resulting in the intensity profile having $2|l|$ intensity maxima, or 'petals'. The angular rotation rate experienced by the intensity profile, as the field propagates along the z-axis, is given by[14,15]

$$\frac{d\theta}{dz} = \frac{k_{2z} - k_{1z}}{2l}. \tag{4}$$

To perform the azimuthal decomposition on such fields, we select a basis that is scale-independent. Such a basis is the angular harmonics, $\exp(il\theta)$, that are orthogonal over the azimuthal coordinate. An expansion of an arbitrary optical field in terms of the angular harmonics is given by[32]

$$u(r,\theta,z) = \frac{1}{\sqrt{2\pi}} \sum_l a_l(r,z) \exp(il\theta), \tag{5}$$

with

$$a_l(r,z) = \frac{1}{\sqrt{2\pi}} \int_0^{2\pi} u(r,\theta,z) \exp(-il\theta) d\theta. \tag{6}$$

The coefficients for the azimuthal modes, a_l, are determined by calculating the inner-product of the initial field, $u(r,\theta,z)$, with a suitable match-filter (phase hologram), $t_l(r,\theta)$. Physically, this requires that the on-axis intensity of the Fourier plane of the initial field, $u(r,\theta,z)$, modulated by the match-filter $t_l(r,\theta)$, be measured[33]

$$U_l(0) = \frac{\exp(i2kf)}{i\lambda f} \int_0^{\infty} \int_0^{2\pi} t_l(r,\theta) u(r,\theta) r dr d\theta. \tag{7}$$

The match-filter has two requirements: it should (i) have an azimuthal phase variation opposite to the mode being analyzed; and (ii) select the information as a function of r. These conditions are satisfied if the match-filter is defined as [30, 33]

$$t_l(r,\theta) = \begin{cases} \exp(-il\theta) & R - \Delta R/2 < r < R + \Delta R/2 \\ 0 & otherwise \end{cases}, \tag{8}$$

which represents an annular ring centered at $r = R$ and of negligible thickness, ΔR.

Measuring the intensity of the signal, $I_l(R,0)$, at the origin in the Fourier plane we obtain the magnitude of the coefficients as

$$a_l(R) = \frac{f}{R\Delta Rk} \sqrt{I_l(R,0)}. \tag{9}$$

Performing the azimuthal decomposition and extracting the phase delays between the azimuthal modes, one can calculate the intensity of the field, $|u(r,\theta)|^2$, the phase and the OAM density[30].

3. EXPERIMENTAL REALIZATION

The experimental setup, depicted in Fig. 2 (a), consists of two parts: (i) the generation of the superimposed higher-order Bessel beams and (ii) the azimuthal decomposition of these rotating fields. A HeNe Gaussian beam was expanded through a 5× telescope before illuminating the liquid crystal display of SLM_1, which was programmed with a digital hologram similar to that in Fig. 1 (b) and Fig. 2 (b), so as to produce a superposition of two OAM carrying Bessel beams. The resulting field is a non-diffracting 'petal' mode (Fig. 2 (c)) that rotates as it propagates[14, 15] and is imaged with a 10x

objective onto SLM_2 for the execution of the azimuthal modal decomposition. The decomposition was accomplished by executing an inner-product of the initial field with the match-filter, $\exp(il\theta)$, for various l values and at particular radial positions. An example of such a match-filter is given in Fig. 2 (d). The on-axis intensity, in the Fourier plane (Fig. 2 (e)) was measured so as to extract the weighting coefficients, a_l.

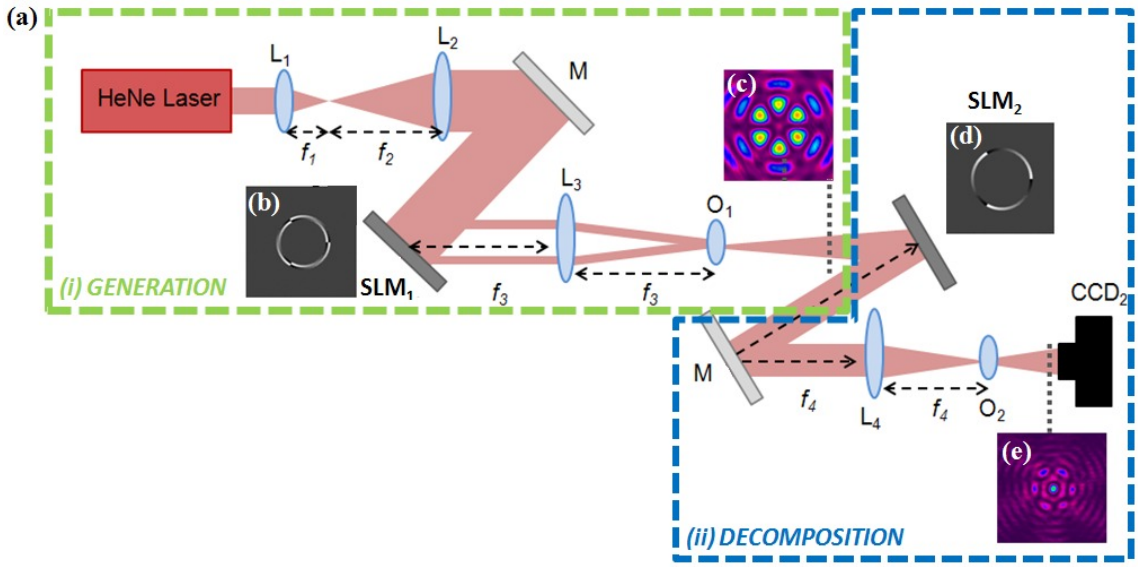

Figure 2. (a) A schematic of the experimental setup for generating the rotating, superimposed Bessel beams and performing the azimuthal decomposition. L: Lens (f_1 = 15 mm; f_2 = 75 mm; f_3 = 200 mm and f_4 = 200 mm); M: Mirror; SLM: Spatial Light Modulator; O: Objective; CCD: CCD Camera. The digital hologram (b) used to generate the rotating optical field (c) and the digital hologram (d) used to extract the azimuthal mode weightings from the inner product (e).

4. RESULTS AND DISCUSSION

The intensity profiles of these non-diffracting, superimposed fields were captured at discrete distances along their propagation and the angular position of a selected 'petal' was calculated for each frame (illustrated in Fig. 3 (a)). The rotation rate of a selected 'petal' was determined from the slope of the straight line that best fits the measured angular position as a function of the propagation distance. Similar slopes (or experimentally measured rotation rates) were obtained for various azimuthal orders, $|l|$, and various differences between the two wave-vectors, Δk. These experimental rotation rates as a function of $|l|$ and Δk are depicted in Figs 3(b) and (c), respectively. Overlaid with the experimental data are the theoretical predictions, represented by dashed lines. An increase in the azimuthal order, $|l|$, results in a hyperbolic decrease in the rotation rate, evident in Fig. 3(b), where the measured rotation rates, for six different values of Δk, are plotted as a function of the azimuthal order $|l|$. Increasing the difference between the two wave-vectors (achieved by increasing the width of the inner and outer annular rings), resulted in the rotation rate of the intensity profile increasing linearly (evident in Fig. 3(c)). Both Figs 3(b) and (c) convey good agreement between the measured data (solid points) and the theoretical predictions (dashed curves).

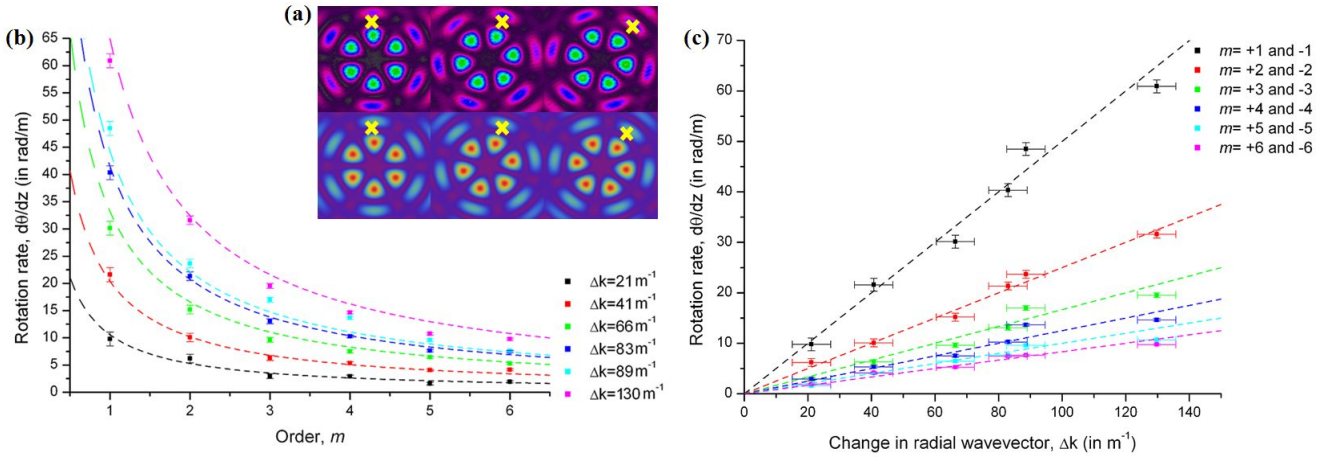

Figure 3. (a) Experimental images (top row) of the intensity profile of a superimposed $l = +3$ and $l = -3$ order Bessel beam, recorded at intervals along its propagation. Corresponding theoretical predictions appear in the bottom row. (b) Graphs of the rotation rates, for fields generated for various differences between the two radial wave-vectors, as a function of the order of the field, $|l|$. (c) Graphs of the rotation rates for beams of various orders $|l|$ as a function of the difference Δk between the two radial wave-vectors.

The match filter was dynamically addressed to consist of an annular ring initially having 10 different radial positions, for azimuthal modes ranging from $l = -4$ to $+4$. The weighting coefficients, a_l, were measured by detecting the on-axis intensity of the inner-product and an example for coefficients, a_{+3} and a_{-3}, as a function of the radial co-ordinate, is given in Fig. 4(a). The example given in Fig. 4(a) is for a superposition of Bessel beams having azimuthal modes of $l = +3$ and -3, resulting in no global OAM. However, the local OAM varies radially across the field for values of $l = +3$ and $l = -3$, evident in Fig. 4(a).

In considering only the azimuthal decomposition of the azimuthal mode $l = +3$, across a superimposed Bessel field possessing azimuthal indices $l = +3$ and -3 for an increased number of annular rings (in this case 46), one can reconstruct the normalized, cross-sectional intensity profile of the field, evident in Fig. 4(b). The cross-sectional intensity profile varies radially across the field (marked by the red arrow), in agreement with the theoretically predicted normalized, cross-sectional intensity profile of a third order Bessel beam (solid black curve). By measuring the phase delays between the azimuthal modes (outlined in Ref. [30]), we found that the entire spatial distribution and phase of the initial field can be reconstructed. The OAM density of the superimposed field was calculated quantitatively, following the analysis outlined in Ref. [33]. In Fig. 4(c) it is evident that the quantitative measurements for the OAM density (given by the red data points) are in very good agreement with the theoretical prediction (blue solid curve). The OAM density, for this particular superposition, oscillates radially across the field, as shown in Fig. 4(c) and its insert.

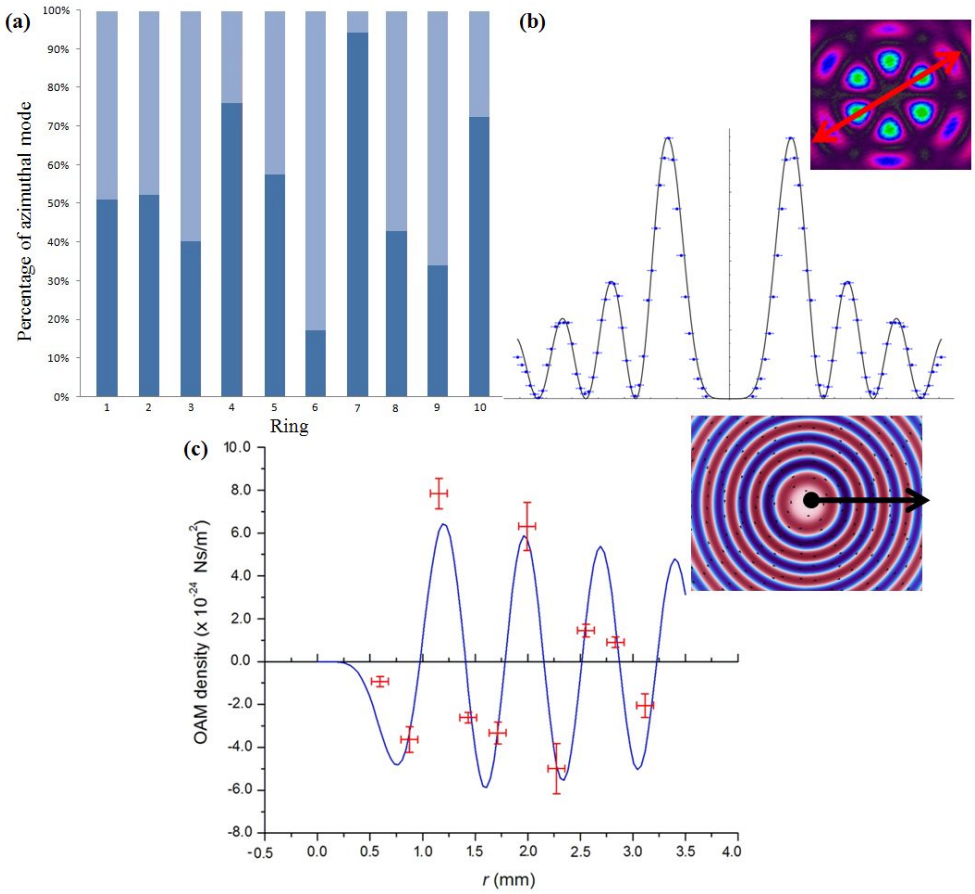

Figure 4. (a) The percentage of the azimuthal mode found at different radial positions (rings 1 to 10) in the field of two superimposed Bessel beams (l =+3 and –3). Light blue denotes the percentage of the azimuthal mode l = +3 and dark blue denotes the percentage of the azimuthal mode l = –3. (b) The cross-sectional intensity profile of the superimposed Bessel beam (insert) extracted when performing an azimuthal decomposition of l = +3 for 46 radial co-ordinates. (c) The measured OAM density (red data points), inferred from the weighting coefficients, a_{+3} and a_{-3}, and the theoretical OAM density (blue curve). The theoretical OAM density distribution (insert). Red denotes negative OAM and blue denotes positive. Light to dark blue denotes an increase in positive OAM and light to dark red denotes an increase in negative OAM.

5. CONCLUSION

We have demonstrated an experimental technique for the production of rotating superpositions of Bessel beams and quantified the angular displacement of the intensity profile as a function of the beam propagation distance. We have shown that by altering the width of the annular rings and the azimuthal modes, encoded in the digital holograms, arbitrarily fine control over the rotation rates of the intensity profile can be achieved, thus making these rotating fields an ideal tool for controlled rotation of trapped particles. We also outlined a simple method for the azimuthal decomposition of an arbitrary field requiring no scale information. Superpositions of two OAM carrying Bessel beams were used as an example to show the reconstruction of the cross-sectional intensity profile and the OAM density. This technique is significant to those working in OAM, both at the classical and quantum level, as well as the emerging field of mode-multiplexing.

REFERENCES

[1] L. Allen, M. W. Beijersbergen, R. J. C. Spreeuw, and J. P. Woerdman, "Orbital angular momentum of light and the transformation of Laguerre-Gaussian laser modes," Phys. Rev. A **45**(11), 8185-8189 (1992).

[2] D. McGloin, K. Dholakia, "Bessel beams: diffraction in a new light," Contemp. Phys., 46, 15-28 (2005).
[3] J. Durnin, J.J. Miceli, and J.H. Eberly, "Diffraction-free beams," Phys. Rev. Lett. **58**(15), 1499-1501 (1987).
[4] R.M. Herman and T.A. Wiggins, "Production and uses of diffractionless beams," J. Opt. Soc. Am. A **8**(6), 932-942 (1991).
[5] J. Arlt and K. Dholakia, "Generation of high-order Bessel beams by use of an axicon," Opt. Commun. **177**(1-6), 297-301 (2000).
[6] J.H. McLeod, "The axicon: a new type of optical element," J. Opt. Soc. Am. **44**(8), 592-597 (1954).
[7] D. McGloin, V. Garces-Chavez, and K. Dholakia, "Interfering Bessel beams for optical micro-manipulation, " Opt. Lett. **28**(8), 657-659 (2003).
[8] J. Turunen, A. Vasara, and A.T. Friberg, "Holographic generation of diffraction-free beams," Appl. Opt. **27**(19), 3959-3962 (1988).
[9] A. Vasara, J. Turunen and A.T. Friberg, "Realization of general nondiffracting beams with computer-generated holograms," J. Opt. Soc. Am. A **6**(11), 1748-1754 (1989).
[10] J.A. Davis, E. Carcole, and D.M. Cottrell, "Nondiffracting interference patterns generated with programmable spatial light modulators," Appl. Opt. **35**(4), 599-602 (1996).
[11] J.A. Davis, E. Carcole, and D.M. Cottrell, "Intensity and phase measurements of nondiffracting beams generated with a magneto-optic spatial light modulator," Appl. Opt. **35**(4), 593-598 (1996).
[12] C. Paterson and R. Smith, "Higher-order Bessel waves produced by axicon-type computer-generated holograms," Opt. Commun. **124**(1-2), 121-130 (1996).
[13] D. McGloin, G.C. Spalding, H. Melville, W. Sibbett, and K. Dholakia, "Three-dimensional arrays of optical bottles," Opt. Commun. **225**(4-6), 215-222 (2003).
[14] R. Vasilyeu, A. Dudley, N. Khilo, and A. Forbes, "Generating superpositions of higher-order Bessel beams," Opt. Express **17**(26), 23389-23395 (2009).
[15] R. Rop, A. Dudley, C. López-Mariscal, and A. Forbes, "Measuring the rotation rates of superpositions of higher-order Bessel beams," J. Mod. Opt. **59**(3), 259-267 (2012).
[16] S. Chavez-Cerda, G.S. McDonald, G.H.C. New, "Nondiffracting beams: travelling, standing, rotating and spiral waves," Opt. Commun. 123, 225-233 (1996).
[17] V.V. Kotlyar, S.N. Khonina, R.V. Skidanov, V.A. Soifer, "Rotation of laser beams with zero of the orbital angular momentum," Opt. Commun. 274, 8–14 (2007).
[18] C. Paterson, R. Smith, "Helicon waves: propagation-invariant waves in a rotating coordinate system," Opt. Commun. 124, 131-140 (1996).
[19] P. Pääkkönen, L. Lautanen, M. Honkanen, M. Kuittinen, J. Turunen, S.N. Khonina, V.V. Kotlyar, V.A. Soifer, A.T. Friberg, "Rotating optical fields: experimental demonstration with diffractive optics," J. Mod. Opt. 45, 2355-2369 (1996).
[20] S.N. Khonina, V.V. Kotlyar, V.A. Soifer, M. Honkanen, L. Lautanen, J. Turunen, "Generation of rotating Gauss-Laguerre modes with binary-phase diffractive optics, " *J. Mod. Opt.* 42, 2, 227-238 (1999).
[21] E. Tervonen, J. Turunen, and A. Friberg, "Transverse laser mode structure determination from spatial coherence measurements: experimental results," Appl. Phys. B **49**, 409-414 (1989).
[22] A. Cutolo, T. Isernia, I. Izzo, R. Pierri, and L. Zerni, "Transverse mode analysis of a laser beam by near- and far-field intensity measurements," Appl. Opt. B **34**, 7974-7978 (1995).
[23] M. Santarsiero, F. Gori, R. Borghi, and G. Guattari, "Evaluation of the modal structure of light beams composed of incoherent mixtures of Hermite-Gaussian modes," Appl. Opt. B **38**, 5272-5281 (1999).
[24] X. Xue, H. Wei, and A. G. Kirk, "Intensity-based modal decomposition of optical beams in terms of Hermite-Gaussian functions," J. Opt. Soc. Am. A **17**, 1086-1091 (2000).
[25] D. Flamm, O. A. Schmidt, C. Schulze, J. Borchardt, T. Kaiser, S. Schroter, and M. Duparre, "Measuring the spatial polarization distribution of multimode beams emerging from passive step-index large-mode-area fibers," Opt. Lett. **35**, 3429-3431 (2010).
[26] T. Kaiser, D. Flamm, S. Schroter, and M. Duparre, "Complete modal decomposition for optical fibers using CGH-based correlation filters," Opt. Express **17**, 9347-9356 (2009).
[27] J. W. Nicholson, A. D. Yablon, S. Ramachandran, and S. Ghalmi, "Spatially and spectrally resolved imaging of modal content in large-mode-area fibers," Opt. Express **16**, 7233-7243 (2008)
[28] D. B. S. Soh, J. Nilsson, S. Baek, C. Codemard, Y. Jeong, and V. Philippov, "Modal power decomposition of beam intensity profiles into linearly polarized modes of multimode optical fibers," J. Opt. Soc. Am. A **21**, 1241-1250 (2004).

[29] M. Paurisse, L. Lévèque, M. Hanna, F. Druon, and P. Georges, “Complete measurement of fiber modal content by wavefront analysis,” Opt. Express **20**, 4074-4084 (2012).
[30] I. Litvin, A. Dudley, F. S. Roux, and A. Forbes, "Azimuthal decomposition with digital holograms," Opt. Express 20(10), 10996-11004 (2012).
[31] D.W.K. Wong, and G. Chen, “Redistribution of the zero order by the use of a phase checkerboard pattern in computer generated holograms,”Appl. Optics **47**(4), 602-610 (2008).
[32] I. Litvin, A. Dudley, and A. Forbes, “Poynting vector and orbital angular momentum density of superpositions of Bessel beams,” Opt. Express 19(18), 16760-16771 (2011).
[33] A. Dudley, I. Litvin, and A. Forbes, “Quantitative measurement of the orbital angular momentum density of light,” App. Opt. 51(7), 823-833 (2012).